

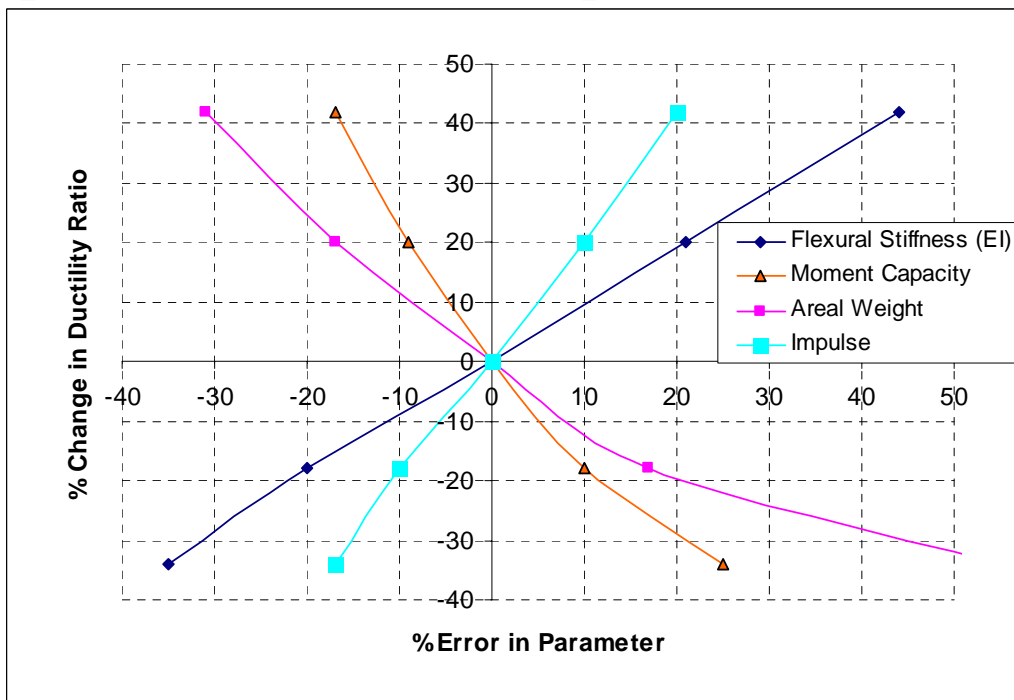


US Army Corps  
of Engineers ®

PDC TR-08-01  
September 2008

## U.S. ARMY CORPS OF ENGINEERS PROTECTIVE DESIGN CENTER TECHNICAL REPORT

### Parameter Study for Single-Degree-of-Freedom Response of Structural Components to Blast Loads



DISTRIBUTION STATEMENT A: Approved for Public Release;  
Distribution is unlimited

## Table of Contents

1.0	Introduction.....	1
1.1	Pressure-Impulse Diagrams.....	1
1.2	CEDAW Methodology.....	3
2.0	Overview of Sensitivity Study.....	5
3.0	Sensitivity of Ductility Ratio Response to Blast Load and Component Properties .....	6
3.1	Sensitivity of Ductility Ratio in the Impulsive Loading Region.....	6
3.1.1	Sensitivity of Ductility Ratio to Ibar.....	6
3.1.2	Sensitivity of Ductility Ratio to Specific Blast Load and Component Properties for Impulsive Response .....	10
3.2	Sensitivity of Ductility Ratio in the Pressure-sensitive Loading Region.....	12
3.3	Sensitivity of Ductility Ratio in the Dynamic Loading Region .....	14
4.0	Sensitivity of Support Rotation Response to Blast Load and Component Properties.....	15
4.1	Sensitivity of Support Rotation in the Impulsive Loading Region .....	15
4.2	Sensitivity of Support Rotation in Pressure-Sensitive Response Realm.....	19
4.3	Sensitivity of Support Rotation in the Dynamic Response Realm.....	20
5.0	Comparison of Sensitivity Study to Results From SDOF Analyses.....	20
6.0	Summary and Conclusions .....	22
7.0	References.....	24

## List of Tables

Table 1. Statistical Summary of Comparison of P-i Diagrams Calculated with CEDAW and SDOF Analyses .....	5
Table 2. Ibar values Causing Impulsive Response in Steel Beams ( $P_{bar} = 25$ ) .....	7
Table 3. Ibar values Causing Impulsive Response in Steel Beams ( $P_{bar} = 7.5$ ) .....	7
Table 4. Summary of Different Ductile Flexural Components Used to Calculate Ibar Values .....	7
Table 5. Calculated Change in Ductility Ratio for Given Changes in Ibar Causing $P_{bar} = 25$ from Figure 4.....	9
Table 6. Change in Ductility Ratio for Given Change in Ibar for Impulsive Response .....	9
Table 7. Sensitivity of Ductility to Ibar for Impulsive Response .....	10
Table 8. Sensitivity of Ductility Ratio to Component and Blast Load Parameters for Impulsive Response .....	10
Table 9. Change in Ductility Ratio for Given Changes in $P_{bar}$ for Pressure-Sensitive Response .....	13
Table 10. Sensitivity of Ductility Ratio to Component and Blast Load Parameters for Pressure-Sensitive Response.....	13
Table 11. Change in Support Rotation for Given Change in $P_{bar}$ for Impulsive Response .....	18
Table 12. Sensitivity of Support Rotation to Component and Blast Load Parameters for Impulsive Response .....	19
Table 13. Change in Ductility Ratio Caused by 25% Increase in Moment Capacity for Different Response Realms.....	21
Table 14. Change in Ductility Ratio Caused by 18% Decrease in Areal Weight for Different Response Realms.....	22
Table 15. Summary Table of Sensitivity Study Results .....	23
Table 16. Independent Blast/Component Parameters .....	24

## List of Figures

Figure 1. Scaled P-i Curves-fits vs. Scaled SDOF Points in Terms of Ductility Ratio for Flexural Response of Steel Beams.....	2
Figure 2. P-i Diagram Considering Response to Only Positive Phase Blast Load.....	3
Figure 3. Comparison of Scaled P-i Curves Based on Ductility Ratio for Steel Beams with Moderate Damage.....	4
Figure 4. Curve-Fit for Relationship Between Ibar and Ductility Ratio for Ductile Flexural Response in Impulsive Response Realm .....	7
Figure 5. Curve-Fit for Relationship Between Ibar and Ductility Ratio for Positive Phase Blast Load Only .....	8
Figure 6. Sensitivity of Ductility Ratio to Component and Blast Load Parameters for Impulsive Response .....	11
Figure 7. Sensitivity of Ductility Ratio to Component and Blast Load Parameters for Pressure-sensitive Response at two Pbar Values .....	14
Figure 8. Sensitivity of Ductility Ratio to Changes in Moment Capacity .....	15
Figure 9. Scaled P-i Curves-fits vs. Scaled SDOF Points in Terms of Support Rotation for Flexural Response of Steel Beams .....	16
Figure 10. Support Rotation Angle.....	17
Figure 11. Curve-Fit for Relationship Between Ibar and Support Rotation for Ductile Flexural Response in Impulsive Response Realm .....	18
Figure 12. Sensitivity of Support Rotation to Component and Blast Load Parameters for Impulsive Response.....	19

## 1.0 INTRODUCTION

The purpose of this study is to investigate the sensitivity of structural component response to the blast load and component property parameters that affect the response in a practical manner as it applies to blast resistant design, rather than developing a comprehensive thesis on the subject. The study is based on the assumption that component response to blast load can be modeled with an equivalent single-degree-of-freedom (SDOF) system, which is typically assumed for blast design. This is important because non-linear dynamic component response is dependent on the component and blast load properties in a manner that is generally very complex.

### 1.1 Pressure-Impulse Diagrams

Pressure-impulse (P-i) diagrams show all the blast loads, in terms of the positive phase peak pressure and impulse of the blast load, causing given levels of component response. The negative phase can be implicitly considered, as in the CEDAW P-i diagrams (Oswald, 2005). Scaled P-i diagrams are especially useful for generalized studies, such as this, because the two blast load parameters are scaled by component properties so that the P-i diagram generally represents the blast loads causing the given response to any component that is consistent with the basic assumptions used to develop the scaling terms. The scaled peak pressure and impulse of the blast load are commonly referred to as  $P_{bar}$  and  $I_{bar}$ , respectively. Available scaled P-i diagrams show all the scaled blast loads causing a wide range of component ductility ratios and support rotations.

Figure 1 shows a scaled P-i diagram for a component with ductile flexural response defined in terms of ductility ratio from the CEDAW methodology. Equation 1 shows the definition of  $P_{bar}$  and  $I_{bar}$ . These terms are derived in large part from conservation of energy equations. Each curve in the scaled P-i diagram shows  $P_{bar}$  and  $I_{bar}$  points representing a full range of blast loads that cause a given level of ductility ratio in a component. The  $P_{bar}$  and  $I_{bar}$  values are calculated using the peak pressure and impulse of the positive phase blast, and the effect of negative phase blast loading is accounted for indirectly through the Y factor in the  $I_{bar}$  term in Equation 1. The Y factor was computationally derived to cause all scaled blast loads (which were calculated with charge weight-standoff cases that included the negative phase), that produced a given level of component response to lie along a single P-i curve (Oswald, 2005).

Impulse-sensitive, or impulsive component response, occurs for all scaled blast loads along the near-vertical sections of the scaled P-i curves in Figure 1. Impulsive response is characterized by a short duration positive phase blast load, on the order of one-third or less of the blast-loaded component's natural period, where the response is largely independent of the peak pressure or shape of the applied blast pressure history. Component response in this region is primarily dependent on the  $I_{bar}$  term. Figure 1 also shows the pressure-sensitive response realm, where the scaled P-i curves have horizontal asymptotes. Component response is primarily dependent only on the peak pressure of blast loads in this region of the scaled P-i diagram. The pressure-sensitive region of the P-i diagram is characterized by blast loads with a very long positive phase duration that causes maximum response well before any negative phase blast load can occur. The

transition region of the scaled P-i diagrams between the impulsive and pressure-sensitive regions of Figure 1 is known as the dynamic region, where component response is influenced by both the peak pressure and impulse of the applied blast load.

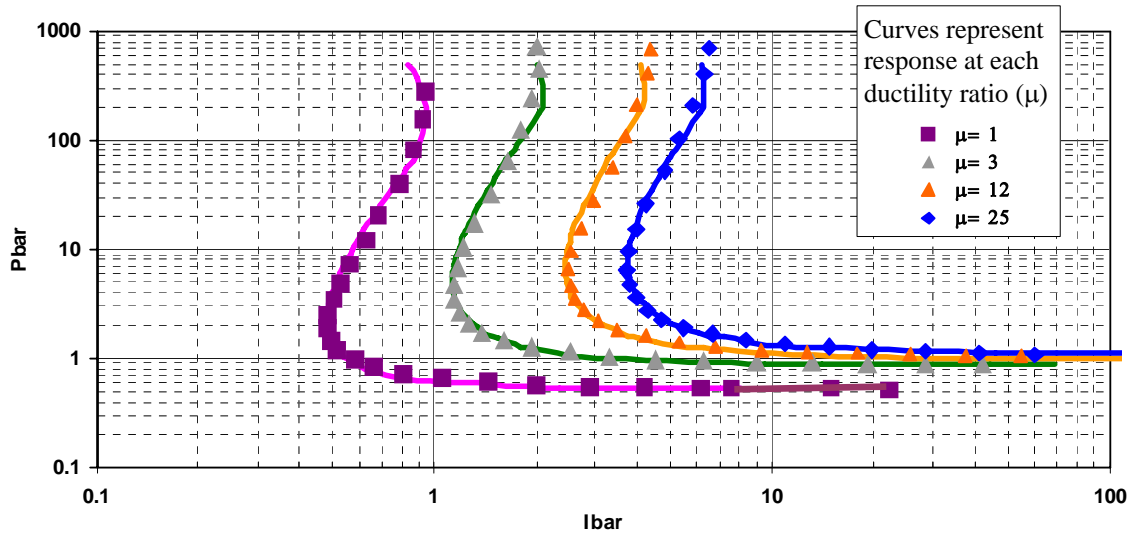


**Figure 1. Scaled P-i Curves-fits vs. Scaled SDOF Points in Terms of Ductility Ratio for Flexural Response of Steel Beams**

$$Pbar = \frac{P}{R_u}$$

$$Ibar = \frac{i}{R_u} \sqrt{\frac{K}{K_{LM} m}} Y = \frac{i}{K_1 M_{du}} \sqrt{\frac{K_2 E I g}{K_{LM} w}} Y$$

$$Y = \frac{Pbar^{(0.5-0.39Rbar^{-0.127})}}{2.59Rbar^{0.067}} \quad Rbar = \frac{R_u}{P_a}$$

**Equation 1**

where:

- P = peak pressure
- i = applied positive phase impulse
- m = mass of equivalent SDOF system for component
- $K_{LM}$  = load-mass factor of equivalent SDOF system for component
- $R_u$  = ultimate flexural resistance of equivalent SDOF system for component at yield
- K = flexural stiffness of equivalent SDOF system for component
- E = modulus of elasticity of component
- I = moment of inertia per unit loaded width of component
- $M_{du}$  = ultimate dynamic moment capacity per unit loaded width of component
- w = areal weight over blast loaded area of component
- g = gravity constant
- $K_1, K_2$  = boundary condition constants for ultimate resistance and stiffness, respectively
- Y = computationally derived term to account for negative phase blast load  
(Note: Y= 1.0 for cases where only positive phase blast loading is considered)
- $P_a$  = atmospheric pressure

Figure 2 shows a scaled P-i diagram where only positive phase blast loading is considered. This P-i diagram is similar to the diagram in Figure 1 except the scaled P-i curves have vertical asymptotes in the impulsive response region. The Pbar and Ibar terms used to generate the curves in Figure 2 are similar to those shown in Equation 1, except there is no Y factor in the Ibar term. The inclusion of negative phase blast loading effects causes the “layover” of the scaled P-i curves in the impulsive response region of Figure 1. The pressure-sensitive region in Figure 2 is essentially identical to that in Figure 1 because the long positive phase blast load durations in this response region of the P-i curves cause maximum response well before any negative phase blast load can occur.

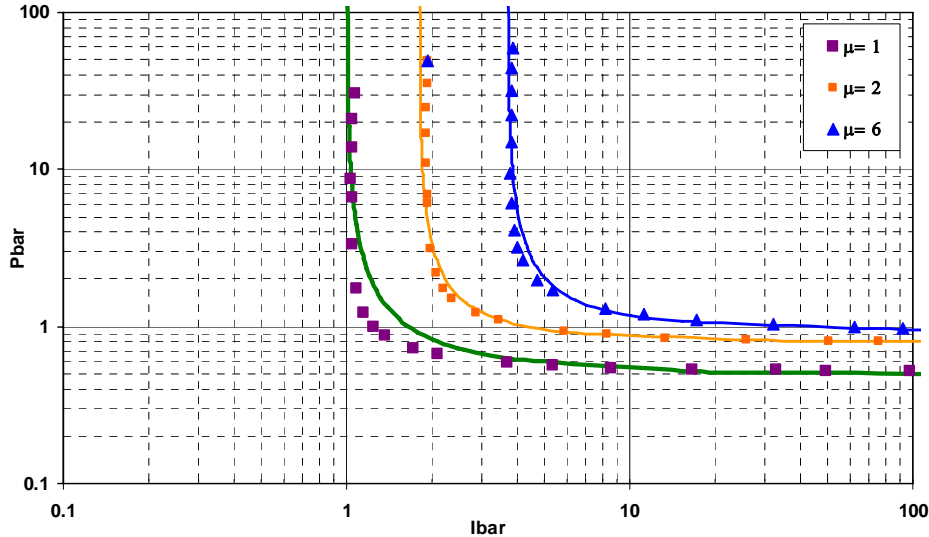


**Figure 2. P-i Diagram Considering Response to Only Positive Phase Blast Load**

## 1.2 CEDAW Methodology

Scaled P-i diagrams similar to, and including Figure 1, were developed for a wide range of different structural component types as part of the development of the CEDAW (Component Explosive Damage Assessment Workbook) procedure to analyze blast-loaded structural components for the U.S. Army Corps of Engineers, Protective Design Center (PDC). The development and accuracy of these scaled P-i diagrams is discussed at length in the CEDAW Methodology Manual (Oswald, 2005). The development is based on theoretical energy balance equations for SDOF response and component response data from several hundred blast tests. The CEDAW P-i diagrams take into account the effect of both positive phase and negative phase blast loading on component response.

Since scaled P-i diagrams from CEDAW will be used in this sensitivity study, it is important to understand their accuracy. The scaled P-i curves allow a very simple, quick analysis of blast-loaded components, but there are several simplifying assumptions and approximations in the development of scaled P-i curves. This includes the development of the scaling equations for Pbar and Ibar, the curve-fit equations used to create the P-i curves, and the fact that negative phase blast load is accounted for in a non-explicit manner. Chapter 7 in the CEDAW Methodology Manual has a detailed discussion on the accuracy of the scaled P-i diagrams. The following paragraphs include a brief summary of this discussion.

The response curves on the scaled P-i diagrams were developed by taking representative components for each component type and using iterative SDOF analyses (similar to those in the SBEDS methodology) to determine a full range of blast loads causing a given response level, then scaling those blast loads by the component properties according to the Pbar and Ibar term equations, and plotting each of the scaled blast loads as a point on the P-i diagram. The P-i curve for the given response level is curve-fit through the scaled points. If the scaling is done properly, the scaled blast load points from many different representative components that all have the same response level should lie on top of each other along a single curve on a P-i diagram.

Numerous checks of this sort were performed and summarized in the CEDAW Methodology Manual, including Figure 3. This figure indicates that the scaling approach is quite accurate for response in terms of ductility ratio since the scaled blast load points from a range of components with very different SDOF properties (as shown at the top of the figure) fall on top of each other. Similar results were obtained for response at other ductility ratios and in terms of support rotation, except slightly more disparity occurred at very high Pbar values above 100 for support rotations. This sensitivity analysis focuses on maximum Pbar values of 25, which are a more realistic upper bound for typical blast design cases.

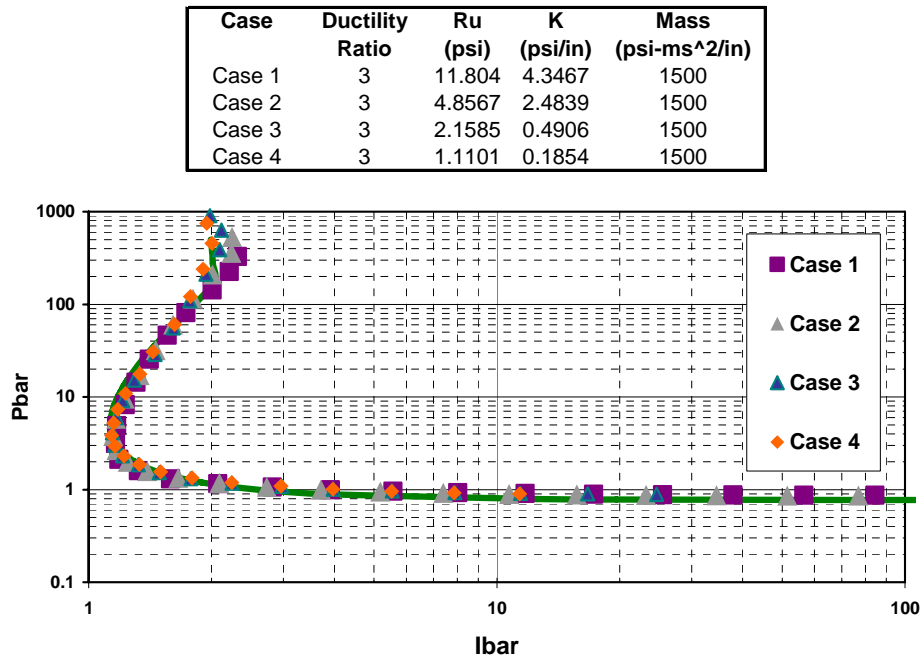


**Figure 3. Comparison of Scaled P-i Curves Based on Ductility Ratio for Steel Beams with Moderate Damage**

Also, the accuracy of the CEDAW scaled P-i diagrams was checked by comparing P-i curves generated with the CEDAW scaled P-i diagrams to P-i curves generated with iterative SDOF-based analyses for the same component and response criteria. Ideally, these P-i curves should match exactly, indicating that the P-i diagrams in CEDAW are as accurate as a time-stepping analysis. The pressure and impulse values calculated with CEDAW were almost always within 15% of comparable values calculated directly with

iterative SDOF-based calculations for flexural response. The only general trend in the comparisons was for CEDAW to slightly overestimate the pressure value of the minimum impulse point on the P-i curves. Table 1 shows a summary of these comparisons. In general, this information indicates that the CEDAW scaled P-i diagrams are accurate enough for this study. The CEDAW Methodology Report (Oswald, 2005) contains more detail.

**Table 1. Statistical Summary of Comparison of P-i Diagrams Calculated with CEDAW and SDOF Analyses**

Statistical Parameter	Pressure Asymptote Comparison	Point of Minimum Impulse Comparison (Dynamic Region)		High Pressure Value Comparison (Impulsive Response Region)
	Pressure Ratio*	Impulse Ratio*	Pressure Ratio*	Impulse Ratio*
Average	0.98	1.10	1.01	0.99
Standard Deviation	0.09	0.17	0.09	0.08

\* Ratio of CEDAW value/SDOF value

## 2.0 OVERVIEW OF SENSITIVITY STUDY

This sensitivity study is based on scaled P-i diagrams from the CEDAW methodology for ductile flexural component response in terms of ductility ratio and support rotations. More complex response modes, such as compression and tension membrane response, are not considered. This study is conducted separately for impulsive and pressure-sensitive component response because of fundamental differences for these two response regions. For example, the mass has no effect on pressure-sensitive SDOF response and therefore SDOF response is independent of the mass for these blast load cases. However, mass does affect impulsive SDOF response. Therefore, a single conclusion of the effect of the mass parameter on SDOF response cannot be obtained. The sensitivity of blast load and component properties for blast load cases in the dynamic region of scaled P-i curves is expected to be bounded by the sensitivity information determined for impulsive and pressure-sensitive component response.

The sensitivity of component response to the blast load and component properties is investigated separately for response in terms support rotation and ductility ratio since these are independent response parameters. Almost all relevant response criteria for blast-loaded components are defined in terms of these two response parameters, indicating that they are both important measures of component response. Also, the sensitivity study focuses on ductile, non-linear (i.e., elastic-perfectly plastic) flexural component response to blast load, which is typically the case for components that are designed to resist blast loads. The sensitivity of blast load and component properties will be studied in the range of +/- 20% from baseline cases because this is a typical range of uncertainty in these parameters for many blast analyses.

Scaled P-i diagrams from CEDAW were initially used in the study to determine the sensitivity of the support rotation and ductility ratio to the Ibar and Pbar terms for impulsive response and pressure-sensitive response, respectively. This relationship was

then extended to specific component blast load and component properties that make up the Pbar and Ibar terms using the mathematical definitions of the Pbar and Ibar terms (see Equation 1). This allows a relationship between a percentage change in specific blast load and component parameters and the corresponding percentage change in response to be determined. Since the study is based on the CEDAW P-i diagrams, which describe response of blast-loaded components in a generalized manner due to the scaling that is used, the results of the sensitivity analysis should also have a general applicability.

### **3.0 SENSITIVITY OF DUCTILITY RATIO RESPONSE TO BLAST LOAD AND COMPONENT PROPERTIES**

As described above, the sensitivity will be investigated separately for the impulsive and pressure-sensitive response regions of SDOF response. The impulsive response region will be addressed first.

#### **3.1 Sensitivity of Ductility Ratio in the Impulsive Loading Region**

Figure 1 shows that impulsive component response occurs for all scaled blast loads along the near-vertical sections of the scaled P-i curves in Figure 1 with Pbar values above approximately 7.5. This Pbar limit of 7.5 is also representative for the limit of impulsive response for other component types, as is shown in Chapter 6 of the CEDAW Methodology Manual (Oswald, 2005). Therefore, Pbar values of 7.5 and greater will be used in this study to represent impulsive response. Component response is primarily dependent on the Ibar term for impulsive response.

##### **3.1.1 Sensitivity of Ductility Ratio to Ibar**

Iterative SDOF analyses were performed for a range of representative structural components to determine the scaled impulse values (Ibar in Figure 1) causing a wide range of ductility ratios for blast loads in the impulsive response realm. This analysis determined all Ibar values causing each ductility ratio of interest for three different specific Pbar values in the impulsive response region of Figure 1. The effect of negative phase blast loads were included in these SDOF analyses as described in the CEDAW Methodology Manual. Table 2 and Table 3 show calculated values of Ibar corresponding to Pbar values of 7.5 and 25 for response at the given ductility ratios for several different steel beam systems. These values can be spot-checked against Figure 1 for the specific ductility ratios that are plotted by going across the plot on a horizontal line where Pbar equals 25 or 7.5 and noting that the Ibar values shown are consistent with the Ibar values on each ductility ratio curve. A similar procedure was used to determine Ibar values corresponding to Pbar = 12.5, but these values fit between those shown in Table 2 and Table 3 and are not shown here. Table 4 shows the wide range of properties of the four different ductile flexural components that were analyzed.

The Ibar values at each ductility ratio causing Pbar values of 7.5 and 25 in Table 2 and Table 3 are nearly the same for all four components that were analyzed. The same was true for the Pbar =12.5 cases. Therefore, the Ibar values are nearly independent of component properties, as expected since the Ibar and Pbar terms in CEDAW were developed to generalize the relationship between component and blast properties and

SDOF response. Curve-fit relationships are developed in Figure 4 between Ibar values and the resulting ductility ratio values based on average Ibar values in Table 2 and Table 3. These relationships are generally applicable for ductile flexural response in the impulsive realm over the realm of SDOF system parameters shown in Table 4.

**Table 2. Ibar values Causing Impulsive Response in Steel Beams (Pbar = 25)**

Component	Ibar Values Cause Causing Pbar =25 Each Ductility Ratio (μ) Value										
	μ = 1	μ = 2	μ = 3	μ = 4	μ = 6	μ = 8	μ = 10	μ = 12	μ = 15	μ = 20	μ = 25
Comp 1	0.69	1.09	1.37	1.60	2.01	2.30	2.57	2.81	3.12	3.58	3.99
Comp 2	0.68	1.09	1.38	1.62	2.01	2.33	2.61	2.86	3.17	3.64	4.07
Comp 3	0.67	1.08	1.37	1.61	2.00	2.33	2.61	2.85	3.17	3.64	4.05
Comp 4	0.64	1.06	1.35	1.60	2.00	2.33	2.62	2.86	3.19	3.66	4.07

**Table 3. Ibar values Causing Impulsive Response in Steel Beams (Pbar = 7.5)**

Component	Ibar Values Cause Causing Pbar =25 Each Ductility Ratio (μ) Value										
	μ = 1	μ = 2	μ = 3	μ = 4	μ = 6	μ = 8	μ = 10	μ = 12	μ = 15	μ = 20	μ = 25
Comp 1	0.55	0.89	1.14	1.34	1.67	1.93	2.17	2.38	2.65	3.06	3.44
Comp 2	0.53	0.89	1.14	1.35	1.68	1.94	2.18	2.39	2.67	3.08	3.46
Comp 3	0.52	0.88	1.15	1.35	1.68	1.95	2.18	2.40	2.68	3.09	3.45
Comp 4	0.51	0.89	1.16	1.37	1.71	1.99	2.22	2.44	2.73	3.14	3.51

**Table 4. Summary of Different Ductile Flexural Components Used to Calculate Ibar Values**

	L (in)	B (in)	Boundary Conditions	Fy (ksi)	Z (in <sup>3</sup> )	I (in <sup>4</sup> )	w (psi)	Ru (psi)	K (psi/in)	Mass (psi-ms <sup>2</sup> /in)	Tn (ms)
Comp 1	360	84	S-S	36	57	310	0.39	2.2	0.5	1002	251
Comp 2	240	60	F-S	50	15	60	0.26	3.7	1.4	684	123
Comp 3	240	60	F-F	50	15	60	0.09	4.9	2.7	234	52
Comp 4	150	60	F-S	50	15	75	0.09	9.5	11.5	234	25

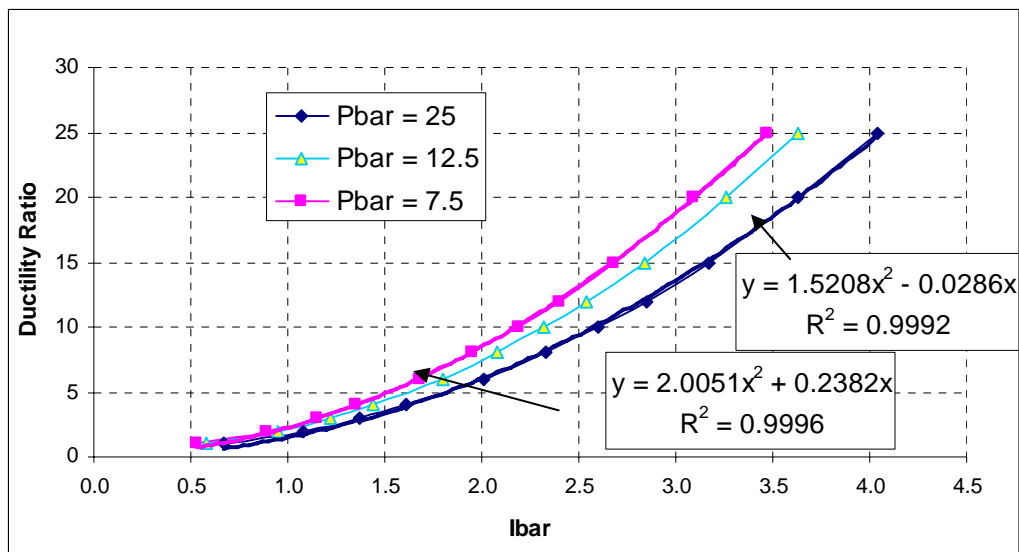


**Figure 4. Curve-Fit for Relationship Between Ibar and Ductility Ratio for Ductile Flexural Response in Impulsive Response Realm**

For any given  $I_{bar}$  of interest, the change in ductility ratio ( $\Delta\mu$ ) caused by a change in  $I_{bar}$  ( $\Delta I_{bar}$ ) can be determined from the curve-fit relationships in Figure 4. This includes the effect of negative phase blast load since this effect is included in the calculations used to determine  $I_{bar}$  values in Figure 4.

Equation 2 shows the energy balance equation (i.e., kinetic energy equal to strain energy) for impulsive response of a component with an elastic-perfectly plastic resistance deflection curve subjected to only positive phase blast load. This equation is algebraically manipulated into a single relationship between the  $I_{bar}$  and ductility ratio for the whole impulsive realm (i.e., all  $P_{bar}$  in the impulsive range). For the case of only positive phase blast load, the P-i diagram has a vertical asymptote in the impulsive realm as shown in Figure 2. Figure 5 shows the relationship between  $I_{bar}$  and ductility ratio from Equation 2 for positive phase blast load only and the curve-fit to this relationship.

$$\frac{i^2}{2K_{LM}m} = R_u \left( x_m - \frac{x_e}{2} \right) \quad \frac{i^2}{K_{LM}mR_u x_e} = 2(\mu - 0.5) \quad \text{Let } x_e = \frac{Ru}{K}$$

$$I_{bar} = \frac{i}{R_u} \sqrt{\frac{K}{K_{LM}m}} = \sqrt{2\mu - 1}$$

$$\mu = 0.5(I_{bar}^2 + 1)$$

See Equation 1 for definition of terms

**Equation 2**

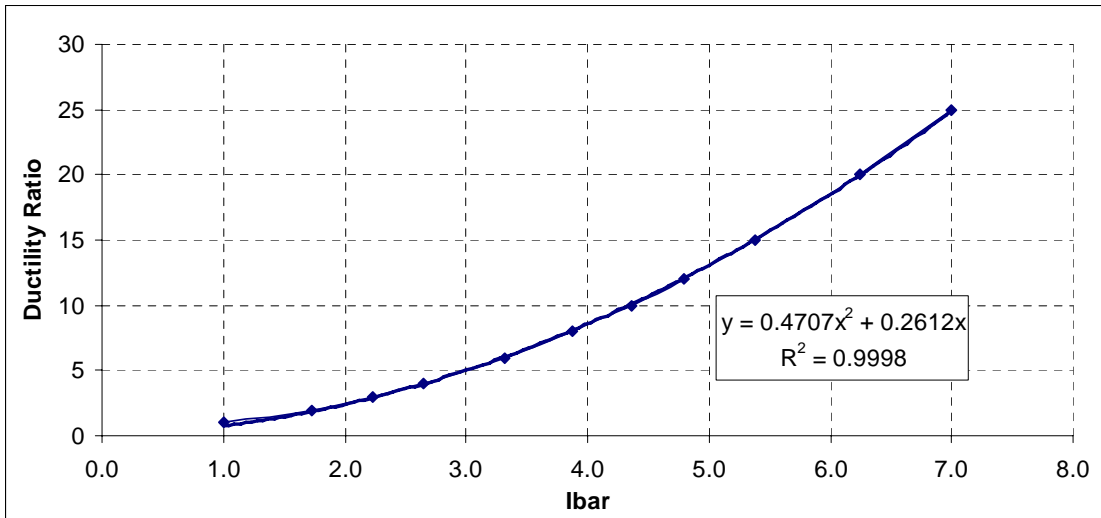


**Figure 5. Curve-Fit for Relationship Between Ibar and Ductility Ratio for Positive Phase Blast Load Only**

The curve-fit relationship for  $I_{bar}$  values causing  $P_{bar} = 25$  in Figure 4 is used to develop Table 5. This table shows detailed information for the calculation of the change in ductility ratio caused by a 20% change (or error) in  $I_{bar}$ . As shown in the table, a 20%

change in Ibar causes a 44% change in ductility ratio for a broad range of ductility ratios typically seen in blast design.

**Table 5. Calculated Change in Ductility Ratio for Given Changes in Ibar Causing Pbar = 25 from Figure 4**

Change in Blast Load or Structural Parameters			Corresponding Change in Response		
Ibar <sub>1</sub>	Ibar <sub>2</sub>	ΔIbar (%)	μ <sub>1</sub>	μ <sub>2</sub>	Δμ (%)
0.80	0.96	20	0.95	1.37	45
1.00	1.20	20	1.49	2.16	44
1.25	1.50	20	2.34	3.38	44
1.50	1.80	20	3.38	4.88	44
1.75	2.10	20	4.61	6.65	44
2.00	2.40	20	6.03	8.69	44
2.25	2.70	20	7.63	11.01	44
2.50	3.00	20	9.43	13.60	44
2.75	3.30	20	11.42	16.47	44
3.00	3.60	20	13.60	19.61	44
3.25	3.90	20	15.97	23.02	44

The same detailed calculations shown in Table 5 were used to determine the percentage change in ductility ratio caused by given percent changes in Ibar in Table 6 for three “Pbar cases”. Each Pbar case consists of the Ibar values which, combined with the given Pbar, cause the full range of ductility ratios shown in the table. The “All” Pbar case represents impulsive response to blast load with only positive phase based on Equation 2 and Figure 2. In this case, the relationship between Ibar and ductility ratio is entirely independent of Pbar (i.e., fully vertical asymptotes as shown in Figure 2) and thus applies to all Pbar. The curve-fit in Figure 5 was used to determine K<sub>Ibar</sub> values. Information is only shown in Table 6 for Ibar values causing ductility ratios between 1 and 25 for each Pbar case since this is the applicable range for almost all blast design.

**Table 6. Change in Ductility Ratio for Given Change in Ibar for Impulsive Response**

Ibar	Change in ductility ratio (Δμ%) for K <sub>Ibar</sub> % change in Ibar											
	K <sub>Ibar</sub> =20%			K <sub>Ibar</sub> =10%			K <sub>Ibar</sub> = -10%			K <sub>Ibar</sub> = -20%		
	All*	Pbar=25	Pbar=7.5	All*	Pbar=25	Pbar=7.5	All*	Pbar=25	Pbar=7.5	All*	Pbar=25	Pbar=7.5
0.80		45	41		21	21		-19	-19		-36	-36
1.00		44	41		21	21		-19	-19		-36	-36
1.25	37	44	42	18	21	21	-16	-19	-19	-31	-36	-36
1.50	38	44	42	18	21	21	-17	-19	-19	-32	-36	-36
1.75	38	44	42	18	21	21	-17	-19	-19	-33	-36	-36
2.00	39	44	43	19	21	21	-17	-19	-19	-33	-36	-36
2.25	39	44	43	19	21	21	-17	-19	-19	-33	-36	-36
2.50	40	44	43	19	21	21	-17	-19	-19	-33	-36	-36
2.75	40	44	43	19	21	21	-17	-19	-19	-33	-36	-36
3.00	40	44	43	19	21	21	-18	-19	-19	-34	-36	-36
3.25	40	44	43	19	21	22	-18	-19	-19	-34	-36	-36
5.0	41			20			-18			-34		
7.0	42			20			-18			-34		

\* These results apply to all Pbar values since they based on based on response to only positive phase blast load. As shown in Figure 2, impulsive response is independent of Pbar for this case.

The results in Table 6 show that nearly consistent results are obtained for all the Pbar cases and percentage changes in Ibar (i.e.,  $K_{Ibar}$  values), where a given percent change in Ibar causes approximately double this percentage change ductility ratio. This is summarized in Table 7. This indicates that the sensitivity of Ibar to ductility ratio is not affected very much by the consideration of negative phase blast load since two of the Pbar cases include this effect and one case (i.e., “All”) does not. The information in Table 6 also shows that the relationship between a percentage change in Ibar and resulting percentage change in ductility ratio is approximately linear over the range of  $K_{Ibar}$  values for each Ibar value. The percentage changes in Ibar in Table 6 (i.e.,  $K_{Ibar}$  values) were selected to represent a range of uncertainty of blast load and component parameter values that is considered most common for blast design.

**Table 7. Sensitivity of Ductility to Ibar for Impulsive Response**

<b>Change in Ibar (%)</b>	<b>20</b>	<b>10</b>	<b>-10</b>	<b>20</b>
<b>Corresponding change in ductility ratio (%)*</b>	42	20	-18	-35
* Approximate average values based on Table 6				

### 3.1.2 Sensitivity of Ductility Ratio to Specific Blast Load and Component Properties for Impulsive Response

Equation 1 shows how Ibar is calculated from specific component and blast load parameters. This information can be used with Table 7 to calculate sensitivity information for ductility ratio to component and blast load parameters. This sensitivity information is shown in Table 8 and plotted in Figure 6. This table and graph show that the change in the calculated ductility ratio is at least proportional to the change in structural and blast parameters affecting pressure-sensitive response, and in some cases it is significantly greater.

**Table 8. Sensitivity of Ductility Ratio to Component and Blast Load Parameters for Impulsive Response**

<b>Change in Ibar (%)</b>	<b>Change in Component/Load Parameters Causing Ibar Change</b>				<b>Change to Ductility Ratio Corresponding to <math>\Delta Ibar</math> (%)</b>
	<b><math>\Delta</math> Impulse (%)</b>	<b><math>\Delta</math> Moment Capacity* (%)</b>	<b><math>\Delta</math> Flexural Stiffness (EI)** (%)</b>	<b><math>\Delta</math> Areal Weight (%)</b>	
20	20	-17	44	-31	42
10	10	-9	21	-17	20
0	0	0	0	0	0
-10	-10	10	-20	17	-18
-20	-17	25	-35	55	-34

\*Resistance boundary condition constant has same sensitivity as moment capacity.  
\*\* Stiffness boundary condition constant has same sensitivity as flexural stiffness.

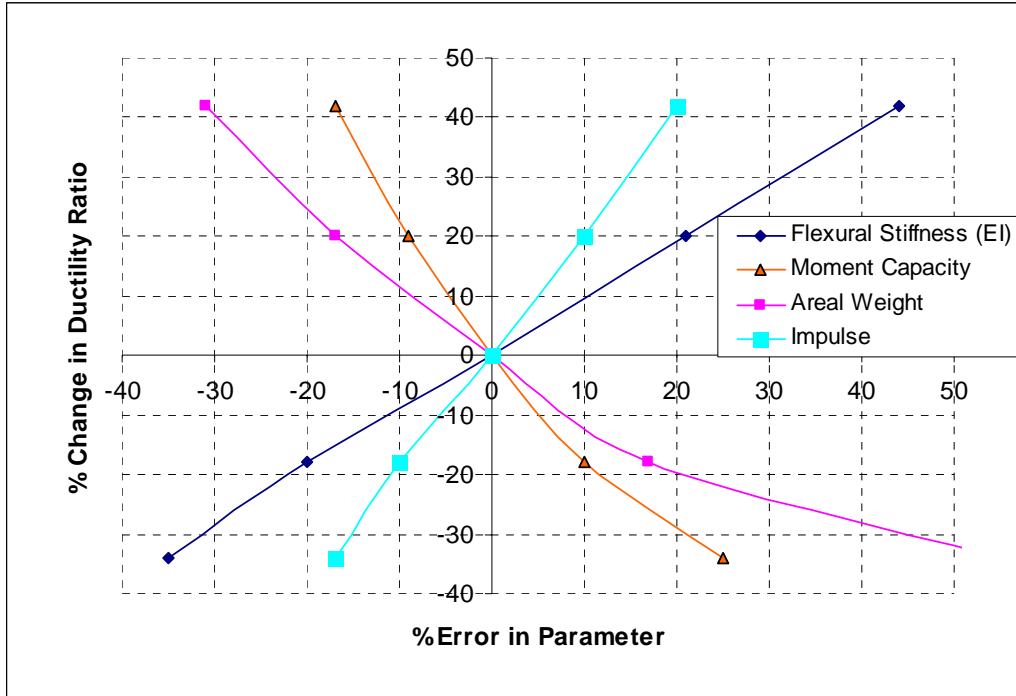


**Figure 6. Sensitivity of Ductility Ratio to Component and Blast Load Parameters for Impulsive Response**

Equation 1 shows that the ultimate resistance, and therefore the moment capacity, is present in both the basic  $I_{bar}$  term and in the  $Y$  factor term that accounts for negative phase blast loading effects. The information in Table 8 and Figure 6 for moment capacity is based only on the basic  $I_{bar}$  term with  $Y=1$  (as applicable for no negative phase blast load). It is very difficult to mathematically establish a sensitivity relationship for the moment capacity including the effect of the  $Y$  factor because of the complexity of the  $Y$  factor term. However, the effect of a given change in the ultimate resistance on the  $Y$  factor term was investigated for this study and the  $Y$  factor is only changed by  $\pm 2\%$  to  $\pm 4\%$  for a  $\pm 20\%$  change in ultimate resistance over a wide range of ultimate resistances from 0.5 psi to 10 psi and for  $P_{bar} = 25$  and  $P_{bar} = 7.5$ . This indicates that it is acceptable for this study to ignore the effect of the  $Y$  factor in the  $I_{bar}$  term when determining sensitivity for the moment capacity, which is the case in Table 8.

As noted in Table 8, the resistance boundary condition constant ( $K_1$  in Equation 1) and stiffness boundary condition constant ( $K_2$  in Equation 1) have the same sensitivity as the moment capacity and the flexural stiffness, respectively. However, this is not very relevant to blast design because theoretical boundary conditions are typically assumed for design and analysis that correspond to discrete cases (i.e., fully fixed or fully pinned). This observation would be more relevant if the rotational restraint at the boundary were explicitly modeled, but this type of modeling is not considered within the scope of “design-based” methodologies for simplified static or dynamic structural design.

### 3.2 Sensitivity of Ductility Ratio in the Pressure-sensitive Loading Region

This same process outlined above in Section 3.1 can also be used to determine the sensitivity of component response (i.e., ductility ratio) for the pressure-sensitive region of SDOF response. The scaled P-i curves in Figure 1 have horizontal asymptotes in this region and the response level is related to Pbar rather than Ibar. As opposed to the impulsive response realm, the negative phase has no effect on component response in the pressure-sensitive region of SDOF response because it occurs at the end of the positive phase blast, very long after peak component response occurs. This greatly simplifies the sensitivity analysis because the relationship between Pbar and resulting ductility ratio can be derived theoretically through a conservation of energy equation (i.e., conservation of work energy and strain energy) as shown to Equation 3. This relationship is applicable for all Ibar values in the pressure-sensitive response region.

$$Px_m = R_u \left( x_m - \frac{x_e}{2} \right) \quad x_e = \frac{R_u}{K} \quad \text{let } \mu = \frac{x_m}{x_e} \quad Pbar = \frac{P}{R_u} = 1 - \frac{1}{2\mu} \quad \text{or} \quad \mu = \frac{1}{2(1 - Pbar)}$$

$$R_u = \frac{K_1 M_{du}}{L^2} \quad \text{therefore} \quad Pbar = \frac{PL^2}{K_1 M_{du}}$$

#### Equation 3

where:

- P = peak pressure
- R<sub>u</sub> = ultimate flexural resistance of equivalent SDOF system for component at yield  
(ultimate resistance based on shear capacity for reinforced concrete columns and connection shear capacity for steel columns)
- M<sub>du</sub> = ultimate dynamic moment capacity per unit loaded width of component
- K<sub>1</sub> = boundary condition constants for ultimate resistance
- L = component span length (twice minimum distance from support to yield line for two-way components)
- x<sub>m</sub> = maximum response of equivalent SDOF system for component
- x<sub>e</sub> = maximum deflection of component at ultimate flexural resistance
- μ = ductility ratio, equal to the ratio of maximum deflection divided by the deflection causing yield at all maximum moment locations

The relationship between Pbar and ductility ratio in Equation 3 is used to determine sensitivity information shown in Table 9. This information shows that the ductility ratio is quite sensitive to Pbar, especially as the Pbar values and the corresponding ductility ratios increase. The information in Table 9 is used along with the relationship between Pbar and specific component and blast load parameters in Equation 3 to determine the information in Table 10. As noted in Table 9, sensitivity information is not shown for cases where the variation in Pbar causes ductility ratios outside the range of 1.0 to 1000 because values outside this range are not of much practical interest in blast resistant design. The information in Table 10 is plotted in Figure 7 for two representative Pbar values of 0.7 and 0.85, corresponding to ductility ratios of 1.7 and 3.3, respectively. This table and graph show that the change in the calculated ductility ratio is at least proportional to the change in structural and blast parameters affecting pressure-sensitive response, and in many cases much greater. The sensitivity of the ductility ratio generally increases as the ductility ratio increases.

**Table 9. Change in Ductility Ratio for Given Changes in Pbar for Pressure-Sensitive Response**

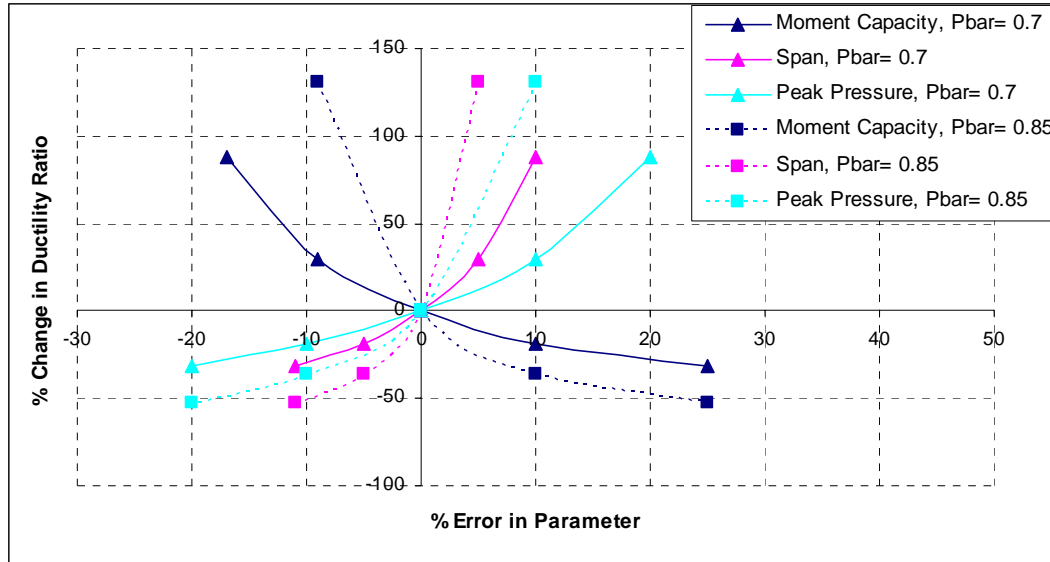
Pbar	Ductility Ratio	% Change in ductility ratio for K% change in Pbar*			
		K=20%	K=10%	K= -10%	K= -20%
0.5	1	25	11	N/A	N/A
0.55	1.1	32	14	-11	N/A
0.6	1.3	43	18	-13	N/A
0.65	1.4	59	23	-16	-27
0.7	1.7	88	30	-19	-32
0.75	2	150	43	-23	-38
0.8	2.5	400	67	-29	-44
0.85	3.3	N/A	131	-36	-53
0.9	5	N/A	N/A	-47	-64
0.95	10	N/A	N/A	-65	-79
0.99	50	N/A	N/A	-91	-95

\* All cases where Pbar < 0.5 or Pbar >=1.0 are marked N/A because they do not correspond to ductility ratios between 1.0 and 1000.

**Table 10. Sensitivity of Ductility Ratio to Component and Blast Load Parameters for Pressure-Sensitive Response**

Ductility Ratio ( $\mu$ )	$\Delta$ Pbar (%)	Changes to Component and Blast Load Parameters corresponding to $\Delta$ Pbar			Change to Ductility Ratio Corresponding to $\Delta$ Pbar (%)
		$\Delta$ Peak Pressure (%)	$\Delta$ Moment Capacity* (%)	$\Delta$ Span Length (%)	
0.55	20	20	-17	10	32
	10	10	-9	5	14
	-10	-10	10	-5	-11
0.7	20	20	-17	10	88
	10	10	-9	5	30
	-10	-10	10	-5	-19
	-20	-20	25	-11	-32
0.85	10	10	-9	5	131
	-10	-10	10	-5	-36
	-20	-20	25	-11	-53

\* Resistance boundary condition constant has same sensitivity as moment capacity



Note: Pbar of 0.7 and 0.85 correspond to ductility ratios of approximately 1.7 and 3.3, respectively.

**Figure 7. Sensitivity of Ductility Ratio to Component and Blast Load Parameters for Pressure-sensitive Response at two Pbar Values**

### 3.3 Sensitivity of Ductility Ratio in the Dynamic Loading Region

Since component response in the dynamic region of scaled P-i diagrams is influenced by both the Ibar and Pbar values (i.e., by both peak pressure and impulse of blast loads), the sensitivity of SDOF response to blast load and component properties are expected to be bounded by, and transition between, the sensitivity information discussed above for the pressure-sensitive and impulsive component response regions. Inspection of Figure 6 and Figure 7 shows that only one of the blast load/component property parameters (i.e., the moment capacity) affects both impulsive and pressure-sensitive response. Figure 8 shows a comparison of how given percentage changes in the moment capacity affect the corresponding ductility ratio for impulsive and pressure-sensitive response. As expected, the ductility ratio is much more sensitive to moment capacity when component response is in the pressure-sensitive response realm. The sensitivity of ductility ratio to other blast load and component properties in the dynamic realm depends on the degree to which the response is closer to either pressure-sensitive or impulse-sensitive response. Several examples will be considered in Section 5.0. Conservatively, the sensitivity of component response in the dynamic region can be based on the sensitivity in either the impulsive or pressure-sensitive response region, whichever causes the more severe sensitivity.

It should be noted that very few high explosive blast loads cause component response in the pressure-sensitive realm, or even very close to this response realm. Only very large explosive amounts (i.e., thousands of pounds) and hundreds of feet standoff distance and industrial explosions (i.e., accidental vapor cloud explosions) typically cause pressure-sensitive response to structural components. Windows are generally the most pressure-sensitive components of buildings. For practical purposes, the sensitivity relationships for ductility ratio on blast load and component property parameters developed for impulsive response are a good indicator of the applicable sensitivity for almost all high explosive loading cases for building components except, possibly, windows.

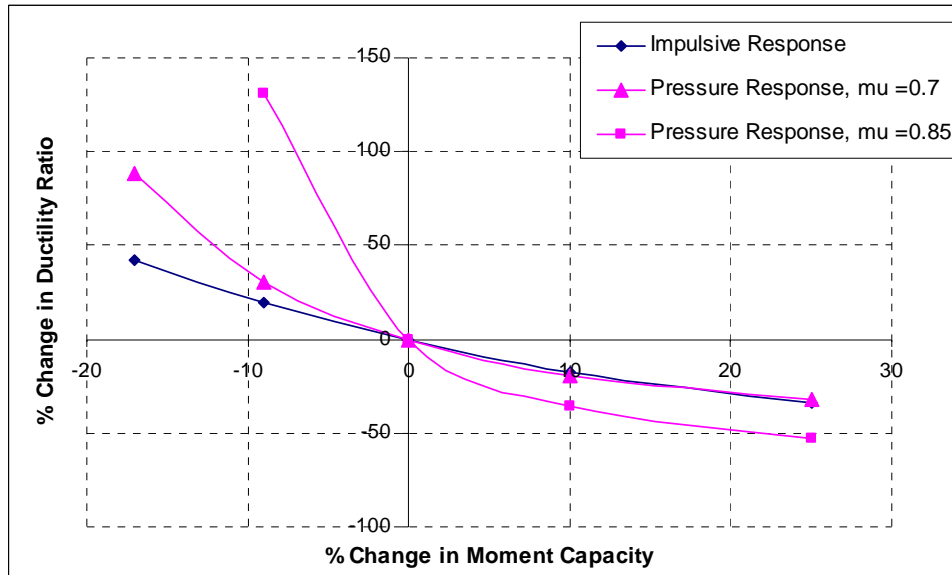


Figure 8. Sensitivity of Ductility Ratio to Changes in Moment Capacity

#### 4.0 SENSITIVITY OF SUPPORT ROTATION RESPONSE TO BLAST LOAD AND COMPONENT PROPERTIES

The whole process outlined above in Section 3.0 to investigate the sensitivity of SDOF response in terms of ductility ratio can be repeated for response in terms of support rotation. Scaled P-i diagrams for component response in terms of support rotation have the same shape P-i diagrams for component response in terms of ductility ratio, but they have different  $P_{bar}$  and  $I_{bar}$  terms. Figure 9 shows a typical scaled P-i diagram from CEDAW for a component with ductile flexural response, where the response is defined in terms of support rotation. Other component types (i.e., other than beams) with ductile flexural response have nearly the same scaled P-i curves for the same support rotation values.  $P_{bar}$  values above approximately 7.5 in Figure 9 are in the “impulsive” response region, where the P-i curves are basically parallel to each other in the vertical direction. Therefore,  $P_{bar}$  values of 7.5 and greater are used in this study to represent impulsive response. This is also true for other component types, as is evident in Chapter 6 of the CEDAW Methodology Manual.

##### 4.1 Sensitivity of Support Rotation in the Impulsive Loading Region

Equation 4 shows the calculation of the  $I_{bar}$  term for impulsive response of a ductile flexural component in terms of support rotation. The calculation is based on an energy balance equation between kinetic energy and strain energy. In the first line of Equation 4, the  $I_{bar}$  term is derived for positive phase blast load. The  $I_{bar}$  term used in Figure 9, which is shown in the second line of the equation, includes the effects of negative phase blast loading through the parameter  $Y$ .

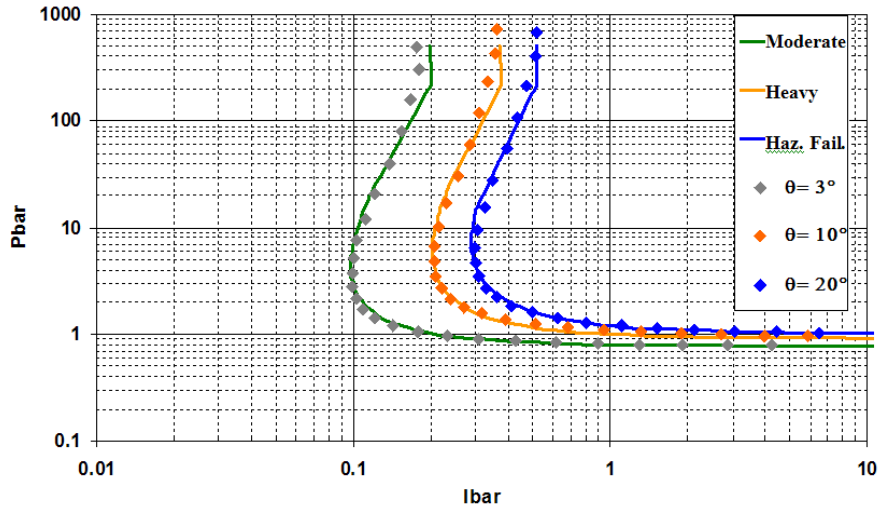


**Figure 9. Scaled P-i Curves-fits vs. Scaled SDOF Points in Terms of Support Rotation for Flexural Response of Steel Beams**

$$\frac{i^2}{2K_{LM}m} = R_u \left( x_m - \frac{x_e}{2} \right) \quad \text{Let} \left( x_m - \frac{x_e}{2} \right) \approx x_m = \theta \frac{L}{2} \quad Ibar = i \sqrt{\frac{1}{K_{LM}mR_uL}} = \sqrt{\theta}$$

$$Ibar = i \sqrt{\frac{1}{K_{LM}mR_uL}} Y \quad \text{including effects of negative phase blast loads}$$

$$R_u = \frac{K_1 M_{du}}{L^2} \quad \text{therefore} \quad Ibar = i \sqrt{\frac{gL}{K_{LM}wK_1M_{du}}} Y$$

#### Equation 4

where:

- $i$  = applied positive phase impulse
- $m$  = mass of equivalent SDOF system for component
- $\theta$  = support rotation (radians) – see Figure 10 below
- $K_{LM}$  = load-mass factor of equivalent SDOF system for component
- $R_u$  = ultimate flexural resistance of equivalent SDOF system for component at yield
- $M_{du}$  = ultimate dynamic moment capacity per unit loaded width of component
- $w$  = areal weight over blast loaded area of component
- $g$  = gravity constant
- $x_e$  = yield deflection
- $x_m$  = maximum deflection
- $K_1, K_2$  = boundary condition constants for ultimate resistance and stiffness, respectively
- $Y$  = see Equation 1

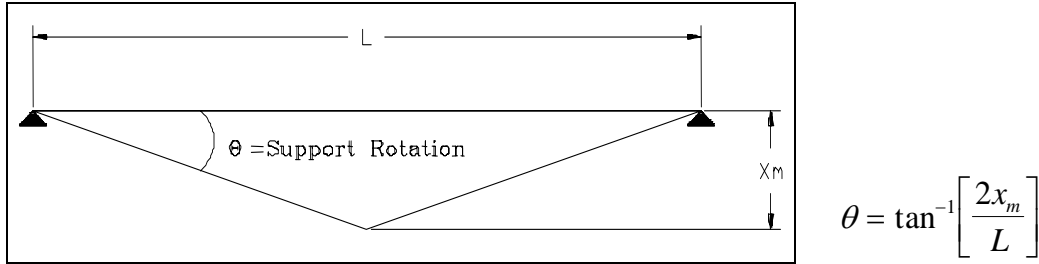


**Figure 10. Support Rotation Angle**

Iterative SDOF analyses were performed for a range of representative structural components to determine the scaled impulse values (Ibar in Figure 9) causing a wide range of support rotations for blast loads with peak pressure having a given Pbar value in the impulsive response realm. This analysis determined all Ibar values causing each support rotation of interest for three different specific Pbar values of 7.5, 12.5 and 25. This was identical to the process explained above in Section 3.1.1. The Ibar values causing each support rotation were calculated for the same four representative structural components in Table 4, and the average Ibar values were plotted against support rotation to develop the curve-fit relationships shown in Figure 11. The Ibar values for any given support rotation in Figure 11 should match the Ibar value along a curve in Figure 9 for the same support rotation at Pbar =25 or Pbar = 7.5. The relationships in Figure 11 show that the support rotation is nearly proportional to Ibar squared, which is similar to the curve-fit relationships between ductility ratio and Ibar in Figure 7 that were also dominated by the Ibar squared term.

The case of positive blast load only is addressed in Equation 4 using the Ibar term with  $Y = 1.0$ . As shown in the first line of the equation, there is a very simple relationship where support rotation is exactly equal to Ibar squared. Since the relationship is so simple, a curve-fit is not required.

Table 11 shows the % change in support rotation caused by given percent changes in Ibar for three “Pbar cases”. Each Pbar case consists of the Ibar values causing that Pbar value for a broad range of support rotations. The Pbar cases are Pbar = 25, Pbar = 7.5, and “All” Pbar (for positive phase only blast load). Nearly consistent results are obtained for all three Pbar cases, where a given percent change in Ibar causes approximately double this percentage change in support rotation for the given range of percentage changes in Ibar. This indicates that the sensitivity of Ibar to support rotation is not affected very much by the consideration of negative phase blast load since two of the Pbar cases include this effect and one case does not. The relationship in Table 11 between a change in Ibar and the resulting change in support rotation is nearly identical to the relationship shown in Table 8 between a change in Ibar and the resulting change in ductility ratio.

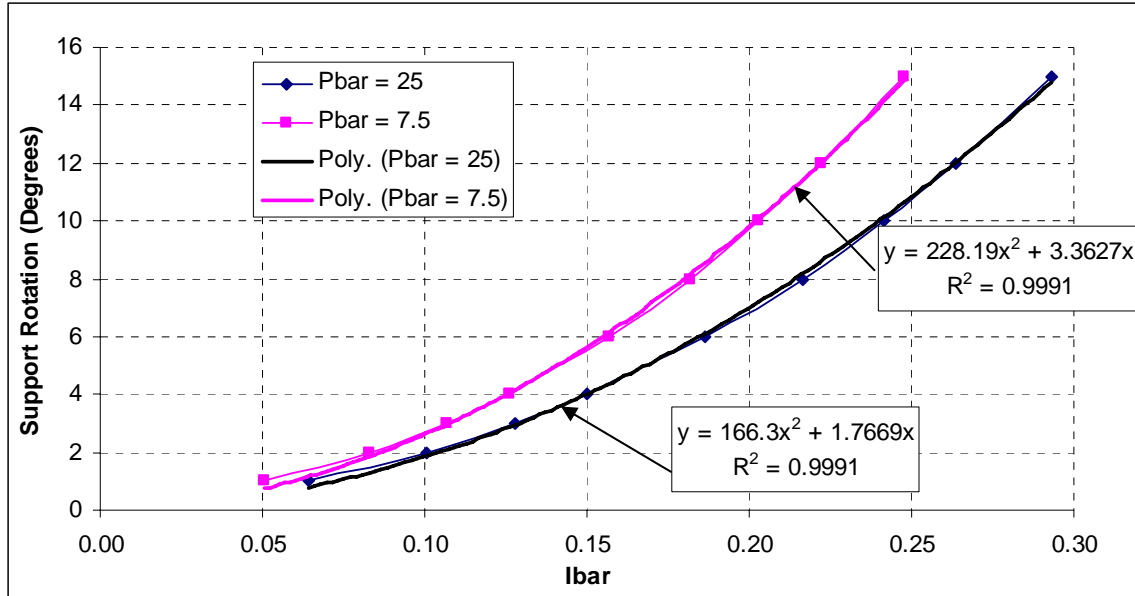


**Figure 11. Curve-Fit for Relationship Between Ibar and Support Rotation for Ductile Flexural Response in Impulsive Response Realm**

**Table 11. Change in Support Rotation for Given Change in Pbar for Impulsive Response**

Ibar	Change in Support Rotation ( $\Delta\theta$ %) for K% change in Ibar											
	K=20%			K=10%			K= -10%			K= -20%		
	All*	Pbar=25	Pbar=7.5	All*	Pbar=25	Pbar=7.5	All*	Pbar=25	Pbar=7.5	All*	Pbar=25	Pbar=7.5
0.15	44	42	42	21	20	20	-19	-18	-18	-36	-35	-36
0.20	44	43	42	21	20	20	-19	-18	-18	-36	-35	-36
0.25	44	43	43	21	21	20	-19	-18	-18	-36	-35	-36
0.30	44	43	43	21	21	20	-19	-18	-19	-36	-35	-36
0.35	44	43	43	21	21	21	-19	-18	-19	-36	-36	-36
0.40	44	43	43	21	21	21	-19	-19	-19	-36	-36	-36
0.45	44	43	43	21	21	21	-19	-19	-19	-36	-36	-36
0.50	44	44	43	21	21	21	-19	-19	-19	-36	-36	-36
0.55	44	44	43	21	21	21	-19	-19	-19	-36	-36	-36
0.60	44	44	43	21	21	21	-19	-19	-19	-36	-36	-36

\* Based on Equation 4 for the case of no negative phase blast load. In this case the results are not sensitive to Pbar region.

The relationship between specific blast load and component property parameters and Ibar in Equation 4 can be used with the information in Table 11 to obtain the information on the sensitivity of support rotation shown in Table 12. The information in Table 12 is plotted in Figure 12.

**Table 12. Sensitivity of Support Rotation to Component and Blast Load Parameters for Impulsive Response**

Change in Ibar (%)	Change in Component/Load Parameters Causing Ibar Change				Change to Support Rotation Corresponding to $\Delta$ Ibar (%)
	$\Delta$ Impulse (%)	$\Delta$ Moment Capacity* (%)	Span Length (%)	$\Delta$ Areal Weight (%)	
20	20	-31	44	-31	43
10	10	-17	21	-17	20
0	0	0	0	0	0
-10	-10	17	-20	17	-18
-20	-17	55	-35	55	-36

\* Resistance boundary condition constant has same sensitivity as moment capacity

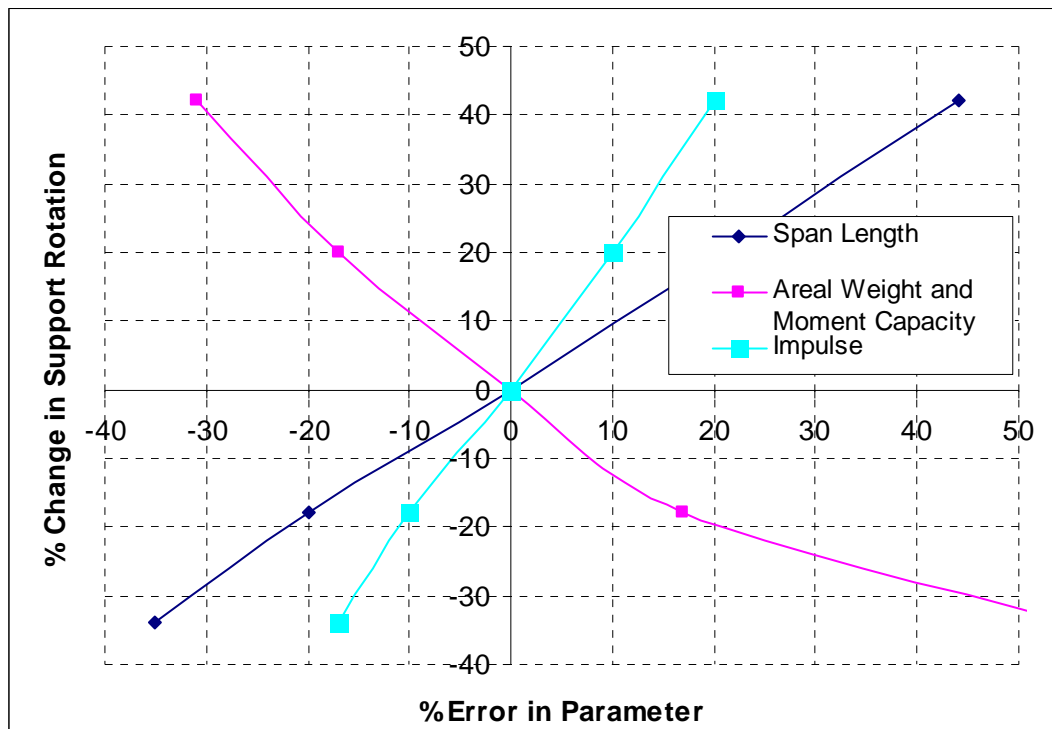


**Figure 12. Sensitivity of Support Rotation to Component and Blast Load Parameters for Impulsive Response**

#### 4.2 Sensitivity of Support Rotation in Pressure-Sensitive Response Realm

Equation 5 shows how the  $P_{bar}$  term is derived from an energy balance equation between work energy and strain energy. Even though the intent is to derive the equation for response in terms of support rotation, it becomes an equation in terms of ductility ratio because the same approximation shown in Equation 4 for  $x_m$  cannot be used in Equation 5 without causing all the response terms to cancel from both sides of the energy balance equation. Equation 5 implies that SDOF response cannot be expressed as a function of support rotation in the pressure-sensitive response realm. It is a function of support rotation only to the extent that the support rotation corresponds for a given component to an “equivalent” ductility ratio that causes the same maximum deflection. This is also

reflected in the fact that the same Pbar term in Equation 1 is used for component response in terms of both ductility ratio and support rotation in CEDAW.

$$Px_m = R_u \left( x_m - \frac{x_e}{2} \right) \quad \text{Let } x_m = \theta \frac{L}{2} \quad Pbar = \frac{P}{R_u} = \frac{\theta \frac{L}{2} - \frac{x_e}{2}}{\theta \frac{L}{2}}$$

$$\text{Let } x_e = \theta_e \frac{L}{2} \quad Pbar = \frac{P}{R_u} = \frac{\theta - \frac{\theta_e}{2}}{\theta} = 1 - \frac{1}{2\mu} \quad \text{since } \mu = \frac{\theta}{\theta_e}$$

*See definitions of terms in Equation 3 and Equation 4*

### Equation 5

Therefore, the basic results in Section 3.2 for the sensitivity of component ductility ratio in the pressure-sensitive response realm also apply to the sensitivity of the support rotation. SDOF response in terms of either support rotation or ductility ratio is very sensitive to the peak pressure and to the component moment capacity and span, which both affect the ultimate resistance ( $R_u$  in Equation 5), especially at high ductility ratios (i.e., greater than 3.0). As explained in the CEDAW Methodology Manual, almost all components that have a Moderate damage level, or greater, have support rotations corresponding to this range of ductility ratios.

#### 4.3 Sensitivity of Support Rotation in the Dynamic Response Realm

The discussion in Section 3.3 for the sensitivity of ductility ratio response to loading in the dynamic response realm is also applicable for the sensitivity of support rotation response in this response realm. Since component response in the dynamic region of scaled P-i diagrams is influenced by both the Ibar and Pbar values (i.e., by both peak pressure and impulse of blast loads), the sensitivity of SDOF response to blast load and component properties are expected to be bounded by, and transition between, the sensitivity information discussed above for the pressure-sensitive and impulsive component response regions. The sensitivity of support rotation to blast load and component properties in the dynamic realm depends on the degree to which the response is closer to either pressure-sensitive, or impulse-sensitive response. Also as discussed in Section 3.2 and 3.3, the sensitivity of SDOF response in the impulsive loading realm is generally more applicable to component response for high explosive blast loading.

## 5.0 COMPARISON OF SENSITIVITY STUDY TO RESULTS FROM SDOF ANALYSES

The SBEDS computer program (Nebuda and Oswald, 2004) was used to make a number of SDOF analyses to test the sensitivity trends noted above. A typical wood stud wall system was used as the basis for this testing. The wall system has No. 2 Southern Pine 2x4 wood studs spanning 8 ft with a 16 inch stud spacing supporting 3 psf of wall material. The wall system had a calculated mass, stiffness, and ultimate resistance values of 71 psi-ms<sup>2</sup>/in, 0.5 psi/in, and 1.25 psi, respectively. Table 13 shows the sensitivity of the ductility ratio ( $\mu$ ) to a 25% change in moment capacity ( $M_{du}$ ) for stud response ranging from impulsive response to pressure-sensitive response, with ductility ratios of

1.5 to 4.0. The type of response transitions from impulsive to pressure-sensitive as the ratio of the blast load positive phase duration ( $t_d$ ) to the component natural period ( $T_n$ ) increases. Only positive phase blast load was considered with no damping except for the two cases in Table 13 noted with an asterisk that had charge weight-standoff blast loads including negative phase blast load. The results from these cases are only a few percent less than those shown in Table 13 for comparable  $t_d/T_n$  cases. This is in agreement with the discussion in Section 3.1.2 that the sensitivity of ductility ratio to moment capacity is not affected very much by the inclusion of negative phase blast load.

**Table 13. Change in Ductility Ratio Caused by 25% Increase in Moment Capacity for Different Response Realms**

Response Realm	$t_d/T_n$ Note 1	$M_{du1}$ (lb-in)	$M_{du2}$ (lb-in)	$\Delta M_{du}$ (%)	P (psi)	i (psi-ms)	$t_d$ (ms)	$\mu 1$	$\mu 2$	$\Delta \mu$ (%)
Impulsive	0.09	22969	28711	25	10.8	32	6	3.04	2.15	-29
Impulsive	0.09 <sup>2</sup>	22969	28711.25	25	17	52	6	4.66	3.44	-26
Impulsive	0.24 <sup>2</sup>	22969	28711.25	25	4.4	35	16	3.07	2.17	-29
Impulsive	0.30	22969	28711	25	4	40	20	3.95	2.66	-33
Dynamic	0.75	22969	28711	25	2	50	50	3.83	2.3	-40
Dynamic	1.79	22969	28711	25	1.35	81	120	3.02	1.68	-44
Pressure Dependent	8.96	22969	28711	25	1.15	345	600	3.93	1.64	-58

Note 1:  $T_n = 67$  ms for all walls  
Note 2: Generated from charge-weight standoff blast load including negative phase blast load

Based on the information in Table 8, a 25% increase in moment capacity should cause a 34% decrease in ductility ratio for impulsive response. Based on information in Table 10 for a  $P_{bar}$  of 0.85, which is consistent with a ductility ratio near 3.0 as shown in Table 13, a 25% increase in moment capacity should cause a 53% decrease in ductility ratio for pressure-sensitive response. The results in Table 13 are therefore consistent with the information in Table 8 and Table 10, and they show how the sensitivity transitions through the dynamic response region.

Table 14 shows results from similar SDOF analyses that investigate the sensitivity of the ductility ratio to an 18% decrease in the areal weight ( $w$ ) of the same stud wall system and same blast loads. Only positive phase blast load was considered with no damping except for the two cases in Table 14 noted with an asterisk that had charge weight-standoff blast loads including negative phase blast load. The results from these cases are consistent other cases shown in Table 14 for comparable  $t_d/T_n$  cases. Based on the information in Table 8 and Table 10, an 18% decrease in areal weight should cause an 18% increase in ductility ratio for impulsive response and it should cause a 0% increase in ductility ratio for pressure-sensitive response. Note in Table 10 that ductility ratio is not dependent on areal weight for pressure-sensitive response. The results in Table 14 are therefore consistent with the information in Table 8 and Table 10, and they show how the sensitivity transitions through the dynamic response region.

This sensitivity analysis focuses on the typical case of SDOF response for components with elastic, perfectly plastic yielding at the maximum moment regions. It is therefore independent of the specific type of component (i.e., steel beam, reinforced concrete

beam, etc.) that has this assumed type of response. This is illustrated by the fact that the results in this section, where wood stud components were used, are consistent previous results, where steel beam components were used.

**Table 14. Change in Ductility Ratio Caused by 18% Decrease in Areal Weight for Different Response Realms**

Response Realm	$t_d/T_n$ Note 1	w1 (psf)	w2 (psf)	$\Delta w$ (%)	P (psi)	i (psi-ms)	$t_d$ (ms)	$\mu 1$	$\mu 2$	$\Delta \mu$ (%)
Impulsive	0.09	71.2	58.4	-18	10.8	32	6	3.04	3.55	17
Impulsive	0.11 <sup>2</sup>	71.2	58.4	-18	11	41	7	3.39	4.07	20
Impulsive	0.24 <sup>2</sup>	71.2	58.4	-18	4.4	35	16	3.07	3.6	17
Impulsive	0.30	71.2	58.4	-18	4	40	20	4.05	4.78	18
Dynamic	0.75	71.2	58.4	-18	2	50	50	3.94	4.5	14
Dynamic	1.79	71.2	58.4	-18	1.35	81	120	3.14	3.37	7
Pressure Dependent	8.96	71.2	58.4	-18	1.15	345	600	3.5	3.59	3

Note 1:  $T_n = 67$  ms for all walls  
Note 2: Generated from charge-weight standoff blast load including negative phase blast load

## 6.0 SUMMARY AND CONCLUSIONS

Scaled P-i diagrams from the CEDAW methodology were used to investigate the sensitivity of ductile flexural component response to blast load and component properties. The scaled P-i diagrams, which generally relate blast loads scaled by component properties to the component response, separate component response into two distinctly different response realms: impulsive-sensitive response and pressure-sensitive response. SDOF response in these regions is dominated by either the impulse or the peak pressure of the blast load, and is also affected by different component properties. Also, separate P-i diagrams relate different blast load and component properties to impulsive response in terms of the two most commonly used response parameters for blast-loaded components: ductility ratio and support rotation. P-i diagrams isolate some of the complexities of SDOF response so that the sensitivities of relevant blast load and component parameters can be studied and understood.

The study was conducted as follows: 1) using iterative SDOF analyses to determine the relationships between a given change in scaled blast load parameters (i.e., Pbar and Ibar) in the CEDAW scaled P-i diagrams and resulting change in component ductility ratio and support rotation, 2) using these relationships, which were specific to the blast loading realm (i.e., pressure or impulse sensitive) and type of response parameter (i.e., ductility ratio or support rotation) to determine the sensitivity of a change in Ibar or Pbar to the resulting change in ductility ratio and support rotation, and 3) using the sensitivity information for Pbar and Ibar to calculate corresponding sensitivity information for the specific blast load and component parameters (i.e., component span length, peak blast pressure, etc.) in the Pbar and Ibar equations. Since the study is based on CEDAW P-i diagrams, it does not consider any gas phase blast loading from internal explosions and is therefore limited to blast loads from external explosions.

Table 15 summarizes the results of the sensitivity study. It should be noted that the study results are not exact. Rather, they are intended to provide trends and a general understanding of the sensitivity of SDOF response to blast load and component parameters. The study shows that, in general, component response changes at least proportionally with changes in relevant blast load and component properties and, in many cases, can change twice as much, or more, than the change in blast load and component properties. The sensitivity of component response varies depending on the particular blast load or component property that is of interest, the extent to which the blast load of interest causes impulsive or pressure-sensitive component response, and the response parameter of interest.

**Table 15. Summary Table of Sensitivity Study Results**

Response Realm <sup>1</sup>	Response Parameter	Building/Load Parameters	Δ Building or Load Parameter (%)	Δ Response Parameter (%) <sup>2</sup>
Impulsive	Ductility Ratio	Impulse	20/-20	42/-40
		Moment Capacity	20/-20	-29/46
		Flexural Stiffness	20/-20	18/-17
		Areal Weight	20/-20	-20/25 -13/20
Pressure	Ductility Ratio <sup>3,4</sup>	Peak Pressure	10/-10	28/-20 (Pbar = 0.7) 130/-35 (Pbar = 0.85)
			20/-20	85/-30 (Pbar = 0.7) >200/-55 (Pbar = 0.85)
		Moment Capacity	10/-10	-20/35 (Pbar = 0.7) -35/145 (Pbar = 0.85)
			20/-20	-25/120 (Pbar = 0.7) -50/>150 (Pbar = 0.85)
		Span Length	10/-10	85/-30 (Pbar = 0.7) >150/-50 (Pbar = 0.85)
		Impulsive	Support Rotation	Impulse
Moment Capacity	20/-20			-20/25
Areal Weight	20/-20			-20/25
Span Length	20/-20			20/-18
Note 1: Sensitivities in dynamic response realm transition between those shown for impulsive and pressure sensitive realms.				
Note 2: The study results in this column are not exact. They are intended to provide trends and a general understanding of the complex sensitivity of SDOF response to blast load and component parameters. Comparable SDOF analyses with variations shown in this table typically calculated about 10% to 30% lower changes in the response parameter than shown above.				
Note 3: Similar sensitivity for support rotations causing ductility ratios greater than 3.0.				
Note 4: Pbar of 0.7 and 0.85 correspond to ductility ratios of approximately 1.7 and 3.3, respectively.				

Pressure-sensitive component response is generally much more sensitive to changes in relevant blast load and component properties than impulsive response, especially at the higher ductility ratios that are typically used in blast design (i.e., ductility ratios greater than 3.0 which typically correspond to the Pbar values shown in the table). The sensitivity of pressure-sensitive component response is a function of Pbar (i.e., the ratio of the peak blast pressure to the ultimate resistance of the blast-loaded component), whereas the sensitivity of impulse-sensitive response is not a strong function of Ibar. The

response of most structural components to high explosive blast loads is more closely approximated as impulsive response. This study also showed that there are some cases, depending on the blast loading realm and the response parameter, where the response is independent of blast/component parameters. These cases are summarized in Table 16.

**Table 16. Independent Blast/Component Parameters**

Response Realm	Response Parameter	Independent Blast/Component Parameter
Pressure-sensitive	Ductility Ratio and Support Rotation	Blast impulse
		Mass
Impulse-sensitive	Ductility Ratio and Support Rotation	Peak blast pressure
	Ductility Ratio	Span
	Support Rotation	Flexural stiffness*
*Only for cases with predominantly plastic response (i.e., ductility ratio greater than approximately 3.0) including most blast-loaded reinforced concrete and reinforced masonry components.		

As indicated in Table 15, the sensitivity of support rotation response for pressure-sensitive component response could not be directly investigated. It was not possible to mathematically relate support rotation to pressure-sensitive response, as was the case for the other cases shown in the table.

Spot checks with comparable time-stepping SDOF analyses using the SBEDS methodology for components with elastic, perfectly plastic flexural yielding, where parameters from Table 15 were varied as shown in the table, generally calculated about 10% to 30% lower changes in the response parameter than those shown in Table 15. This is probably due to the approximations involved in the scaled P-i diagrams compared to the more accurate time-stepping solution used in SDOF analyses. However, all the same trends shown in Table 15 were evident in the SDOF analyses.

Finally, this study indicates that the sensitivity of blast load and component properties is not affected very much by the consideration of negative phase blast load since cases that included this effect and those that did not had similar results. Also, the sensitivities of support rotation and ductility ratio to blast load and component properties were generally linear over the response range that was studied (i.e., +/-20%).

## 7.0 REFERENCES

Nebuda, D. and Oswald, C.J., "SBEDS (*Single degree of freedom Blast Effects Design Spreadsheets*)," Proceedings from the 31st DoD Explosives Safety Seminar, San Antonio, Texas, August, 2004.

Oswald, C.J., "*Component Explosive Damage Assessment Workbook (CEDAW)*," Prepared by Baker Engineering and Risk Consultants for the U.S. Army Corps of Engineers Protective Design Center, Contract No. DACA45-01-D-0007-0013, May, 2005.